In-situ DRIFTS measurements for the mechanistic study of NO oxidation over a commercial Cu-CHA catalyst☆

Maria Pia Ruggeri[a], Isabella Nova[a], Enrico Tronconi[a,*], Josh A. Pihl[b], Todd J. Toops[b], William P. Partridge[b]

[a] *Laboratory of Catalysis and Catalytic Processes, Dipartimento di Energia, Politecnico di Milano, Piazza Leonardo da Vinci 32, I-20133, Milano, Italy*
[b] *Fuels, Engines, and Emissions Research Center, Oak Ridge National Laboratory, 1 Bethel Valley Road, Oak Ridge, TN 37831, USA*

Received 25 July 2014
Received in revised form 21 October 2014
Accepted 29 October 2014
Available online 3 November 2014

1. Introduction

Selective Catalytic Reduction (SCR) is an effective technology that is nowadays widely employed for the abatement of NO_x emissions from mobile sources, such as diesel vehicles. The technology is based on the use of NH_3 for NO_x reduction, which can occur via various reactions. The Standard SCR reaction (1),

$$2NH_3 + 2NO + \frac{1}{2}O_2 \rightarrow 2N_2 + 3H_2O \quad (1)$$

as well as the Fast SCR (2) and the NO_2 SCR (3) reactions

$$2NH_3 + NO + NO_2 \rightarrow 2N_2 + 3H_2O \quad (2)$$

$$2NH_3 + \frac{3}{2}NO_2 \rightarrow \frac{7}{4}N_2 + 3H_2O \quad (3)$$

globally account for the NH_3–NO_x reactivity in modern SCR converters, which are based on metal (Cu, Fe)-exchanged zeolite catalysts. The Fast SCR reaction (2) is of particular interest, since it enables high NO_x conversions at low temperatures. Several literature studies on both V-based [1–4] and metal-promoted zeolite catalysts [5–8] have unveiled the redox nature of the Fast SCR mechanism, whose rate is enhanced by the presence of strongly oxidizing species like NO_2 and surface nitrates: nitrates reduction by NO has been identified as the key step of the process [1–4]. The Standard SCR mechanism, on the contrary, has been the object of controversial proposals [9–11] in which the overall Standard SCR (1) chemistry would result from a consecutive two-step mechanism involving first the slow NO oxidation to NO_2,

$$NO + \frac{1}{2}O_2 \rightarrow NO_2 \quad (4)$$

* Corresponding author. Tel.: +39 02 2399 3264; fax: +39 02 2399 3318.
E-mail address: enrico.tronconi@polimi.it (E. Tronconi).

followed by the fast SCR (2) reaction. However, some of us have recently reported multiple kinetic evidence which shows that NO oxidation to gaseous NO_2 can hardly be the rate determining step of the Standard SCR over Cu- and Fe-promoted zeolites. Instead, an alternative pathway has been proposed in which the NO oxidation and the Standard SCR mechanisms share nitrite-like species as oxidized intermediates [12].

The present paper describes a DRIFTS (diffuse reflectance infrared Fourier transform spectroscopy) in-situ study of a commercial Cu-exchanged chabazite (Cu-CHA) catalyst aimed at investigating the nature and the reactivity of surface species involved in the NO oxidative activation, with the purpose of providing new mechanistic insights and elucidating its relationship with the mechanism of the Standard SCR reaction. Moreover, we present dedicated bench reactor experiments aimed at the investigation of the consistency between the proposed mechanism for NO oxidation and the kinetic effects of water, oxygen and NO_2 concentrations on the NO oxidation activity. A dedicated paper reporting an analogous study of the Standard SCR mechanism on the same Cu-CHA catalyst will follow.

2. Experimental

2.1. Catalyst

Experiments were performed on a commercial Cu-CHA catalyst made by BASF Corporation and used on light duty diesel vehicles in the USA. Details of the catalyst composition, performance, and aging behavior were published by Schmieg and coworkers [13]. Briefly, the CHA zeolite is an aluminosilicate with a nominal silica to alumina ratio of 35:1. CHA is 100% ion exchanged with copper, resulting in a copper loading of 2.8 wt% (expressed as copper metal). The exchanged zeolite is coated on a cordierite flow-through monolith substrate.

2.2. DRIFTS experimental equipment

A sample slab composed of a thin layer of washcoat supported on cordierite was cut from the original honeycomb monolith catalyst. The area of the sample was approximately 0.8 cm^2, in order to fit in the specially designed in-situ DRIFTS reactor cell. The reactor consisted of a stainless-steel cell with an integral cartridge heater functioning as the sample holder. The sample temperature was measured by a type K thermocouple in direct contact with the catalyst sample, and temperatures up to 550 °C were achievable. The reactor cell was operated below atmospheric pressure (500 Torr) to seal a removable zinc selenide (ZnSe) hemispherical dome to the top of the reaction cell with a perflouro-elastomer gasket. The DRIFTS measurement system consisted of a Harrick Scientific ellipsoidal mirror DRIFTS accessory coupled with a MIDAC model M2500 FTIR spectrometer. The ellipsoidal mirror geometry enabled maximum detection of light diffusely scattered at all azimuthal angles from the sample surface to assure high signal to noise ratios. The IR light was transmitted to and from the sample surface through the removable hemispherical dome of spectral-grade ZnSe. A mercury–cadmium–telluride (MCT) detector was used to collect the IR light. A more detailed description of the equipment is provided by Toops et al. [14,15].

Mass flow controllers were used to set NO, NO_2, O_2 and Ar feeds. A saturator immersed in a recirculating constant temperature bath was used to control the H_2O feed concentration. Two 4-way switching valves allowed step changes in the composition feed in order to perform O_2 and NO_x pulses, while keeping the total volumetric flow through the reactor cell constant.

Each spectrum was collected by averaging 8 scans with a 2 cm^{-1} resolution. The choice of collecting 8 scans/spectrum ensured a high temporal resolution while maintaining reasonable signal-to-noise ratio. For each series of spectra, after an oxidizing or reducing pre-treatment of the catalyst sample and prior to introducing the reactive gases, a background spectrum was recorded under Ar or Ar + H_2O at the experiment temperature. The background was then used as a reference for the data conversion to absorbance units.

2.3. Sample pre-treatment and test conditions

Before each experiment, the sample was pre-treated for 1 h at 500 °C in 100 STP cm^3/min Ar flow, using either 8% O_2 (oxidizing pre-treatment) or 1000 ppm NH_3 (reducing pre-treatment). In the case of a reducing pre-treatment, the catalyst was cooled down in Ar to the desired temperature; in the case of oxidizing pre-treatment, oxygen flow was maintained until the sample reached the experiment temperature and was then removed from the gas phase before beginning the experiment. Due to the main interest in understanding the low-temperature NO activation mechanism, the experiments have been focused in the 120–200 °C region. Moreover, the DRIFTS technique is limited by high temperatures, since the IR wavelengths are affected by thermal radiation. In addition, the low reaction rates and the greater thermodynamic stability of adsorbed species at low temperatures guaranteed a high concentration of surface species for DRIFTS analysis. The gas mixtures fed to the reactor cell contained 500 ppm of NO or NO_2 and 0–8% of O_2. Measurements with 1% H_2O in the gas mixture were used in an experiment dedicated to studying the effect of water on NO_x adsorption. NO_x adsorption experiments lasted for 20 or 30 min, depending on the species, in order to reach steady-state surface concentrations. At the end of the adsorption step, the catalyst was purged in Ar at constant temperature to assess the surface species stability.

2.4. Bench reactor kinetic experiments

Additional kinetic runs were performed in a bench flow reactor to investigate the NO oxidation and Standard SCR activity of the commercial Cu-CHA catalyst. Core monolith samples (1.18–3 in.) were cut from the original commercial monolith and then wrapped in a fiber glass insulation tape to minimize gas flow bypass of the catalyst, before being inserted in a quartz tube placed in the reactor furnace. A K-type thermocouple was inserted at the mid-length of the monolith from the reactor outlet to measure the catalyst temperature. To prevent axial temperature gradients, quartz rods were placed in the reactor tube both upstream (for gas preheating and premixing) and downstream the catalyst samples. Gases were supplied by mass flow controllers and were preheated and premixed in a coiled tubing enclosed in a separate preheater furnace before entering the flow reactor. All the gas lines were kept at a temperature higher than 200 °C. Gas analysis relied on a high-speed FTIR gas analyzer (MKS) which provides temporally resolved species profiles by measurements of NO, NO_2, NH_3 and N_2O.

The activity of NO oxidation was studied between 150 and 350 °C, far from thermodynamic equilibrium. A GHSV corresponding to 30000 h^{-1} referred to an equivalent volume of monolith (Q = 4985 Ncc/min; W_{cat} = 3.98 g) was set using N_2 as balance gas, and feed gas concentrations were varied to study the effects of H_2O, O_2 and NO_2: 2–8% O_2, 0–8% H_2O, 0–500 ppm of NO, 0–500 ppm of NO_2. In addition, the standard SCR activity was investigated at a GHSV = 90000 h^{-1} (Q = 14955 Ncc/min; W_{cat} = 3.98 g) between 150 and 250 °C: such experimental conditions were chosen in order to

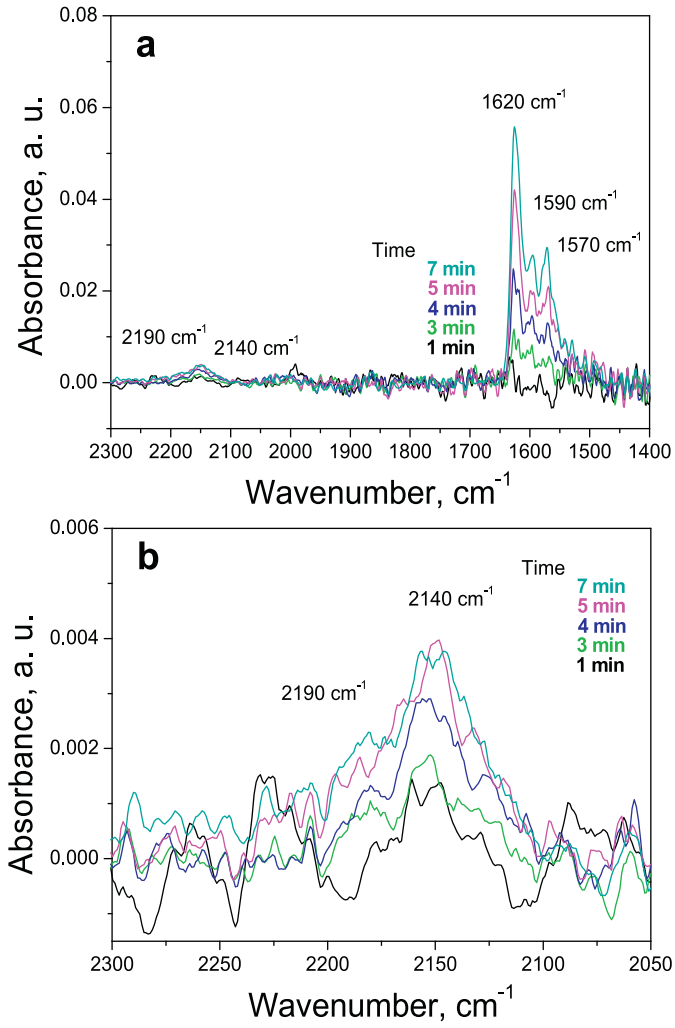

Fig. 1. NO_2 adsorption at 150 °C on pre-oxidized catalyst: DRIFT spectra collected after 1, 3, 4, 5 and 7 min; (a) 2300–1400 cm^{-1} region and (b) 2300–2050 cm^{-1} region.

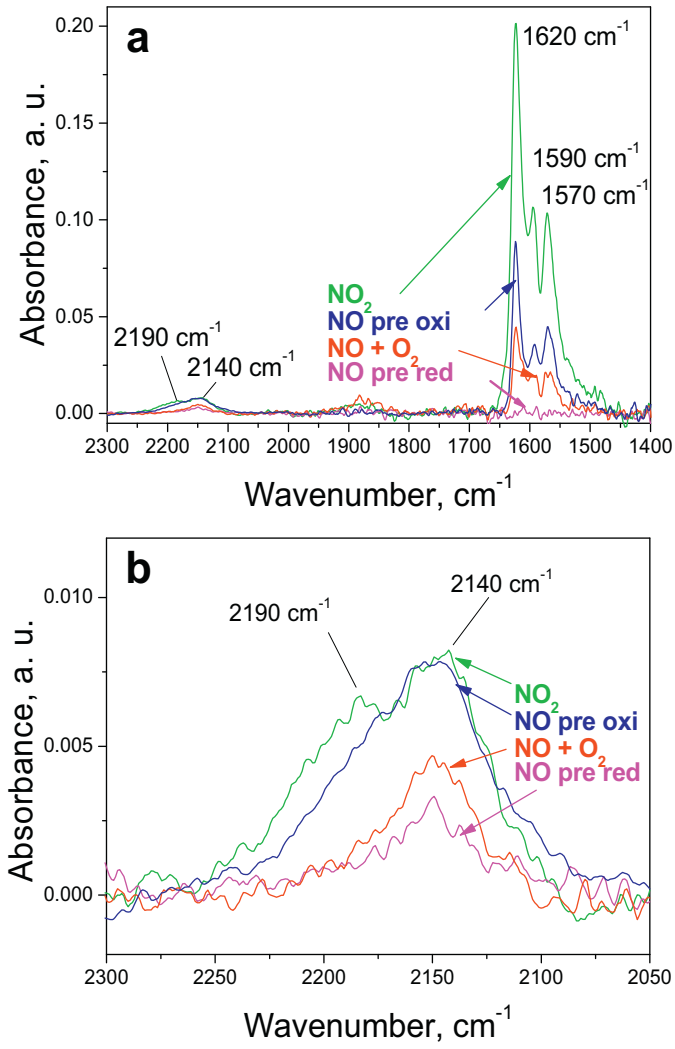

Fig. 2. DRIFT spectra for NO_x adsorption at 150 °C after 20 min: NO_2 on pre-oxidized catalyst, NO adsorption on pre-oxidized catalyst, NO + O_2 adsorption on pre-reduced catalyst, NO adsorption on pre-reduced catalyst; (a) 2300–1400 cm^{-1} region and (b) 2300–2050 cm^{-1} region.

avoid complete conversion, since Cu-CHA catalysts are known to exhibit high SCR performance [12,16].

3. Results and discussion

3.1. NO_x adsorption: identification of surface species

3.1.1. NO_2 adsorption

Fig. 1 shows the temporal evolution of DRIFTS spectra collected during NO_2 adsorption at 150 °C on a pre-oxidized catalyst. The sample pre-treatment included exposure to 8% O_2 for 1 h at 500 °C and during the cool down to 150 °C: oxygen was then removed from the gas phase before feeding NO_2. Upon NO_2 adsorption, bands located in the 1700–1400 cm^{-1} and in the 2200–2100 cm^{-1} spectral regions appear already after 1 min and then progressively grow in intensity (Fig. 1a). In the 1700–1400 cm^{-1} range, multiple bands are present, including three distinct peaks centered at 1620, 1590 and 1570 cm^{-1}. The height of these three bands increases at the same rate. Since the intensity of the 2200–2100 cm^{-1} bands is one order of magnitude smaller than the 1700–1400 cm^{-1} peaks, Fig. 1b magnifies the 2300–2050 cm^{-1} spectral region to enable a closer analysis of this portion of the spectra. A broad symmetric peak, centered at 2140 cm^{-1} is already visible after 3 min. Moreover, a shoulder at 2190 cm^{-1} appears in the spectra after 5 min.

3.1.2. NO adsorption

Fig. 2 compares the spectrum for NO_2 adsorption at 150 °C on the pre-oxidized catalyst, obtained after 20 min, with spectra collected during three NO adsorption experiments, respectively, on a pre-oxidized catalyst, on a pre-reduced catalyst, and on a pre-reduced catalyst in the presence of O_2, all at the same temperature and adsorption time. With the single exception of the NO adsorption on the pre-reduced catalyst, the spectra collected during NO_x adsorption share the same features in the 1700–1400 cm^{-1} region (Fig. 2a), wherein three distinct peaks can be distinguished, located at 1570–1590–1620 cm^{-1}. As more clearly shown in Fig. 2b, additional bands are located around 2140 and 2190 cm^{-1}. In this case, for NO_2 adsorption, the 2190 cm^{-1} feature is more prominent than in the spectra collected at earlier adsorption times shown in Fig. 1b. In the following, NO_x adsorption results are analyzed in detail to identify possible differences or specific features of the above-mentioned bands depending on the gas feed composition and the catalyst oxidation state.

a) NO + O_2 adsorption on pre-reduced catalyst

When the adsorption of 500 ppm NO in the presence of 8% O_2 is carried out on a pre-reduced catalyst at 150 °C for 20 min,

the same bands located both in the 1700–1400 cm^{-1} and in the 2200–2100 cm^{-1} region, but no shoulder at 2190 cm^{-1} is observed, as during NO_2 adsorption. The intensity of the bands is however much lower.

b) NO adsorption on pre-reduced catalyst

As apparent from Fig. 2a, no bands in the 1700–1400 cm^{-1} region are detected when only 500 ppm of NO are fed to a pre-reduced catalyst. Only a broad symmetric band, centered at 2140 cm^{-1}, is observed, whose peak intensity is, however, very low.

c) NO adsorption on pre-oxidized catalyst

The same features observed in the case of NO_2 and $NO + O_2$ adsorption are apparent when NO is adsorbed for 20 min at 150 °C on a pre-oxidized catalyst. Bands located at 1570–1590–1620 cm^{-1} are detected: their intensity is lower than in the case of NO_2 adsorption, but higher than during $NO + O_2$ adsorption on a pre-reduced catalyst. The same is observed for the 2140 cm^{-1} band. Only a very small shoulder at 2190 cm^{-1} is noted in this case.

Identification of surface species

The bands in the 1700–1400 cm^{-1} region, observed in all the NO_x adsorption runs with the exception of NO adsorption on a pre-reduced catalyst, are typically assigned to nitrate species formed on Cu sites [17–19]. In particular, the peak located at 1620 cm^{-1} can be assigned to a bridging nitrate complex, which would require two adsorption sites, whereas the 1590–1570 cm^{-1} band can be attributed to bidentate nitrates [20]. Our results in Fig. 2 show that such nitrates can be formed either from gas phase NO_2 or $NO + O_2$. Moreover, it has been shown that nitrates can be formed from NO without gas phase oxygen, provided that the catalyst has been pre-oxidized.

The identification of the band centered around 2140 cm^{-1} is, on the contrary, not trivial. This band was assigned to NO_2^+ by Szanyi et al. [21] who pointed out that this species could be generated on H-ZSM-5 by the interaction of NO_2, formed in $NO + O_2$ presence, with Brønsted acid bridging hydroxyl groups; this band was not detected on Cu-ZSM-5, in which the above-mentioned hydroxyl groups are substituted by Cu in the exchange process. Later, Hadjiivanov et al. [22,23] demonstrated by labeled O_2 experiments that the 2133 cm^{-1} band observed under $NO + O_2$ adsorption on H-ZSM-5 is not due to NO_2^+ and concluded that it can be assigned to NO^+ (nitrosonium ions) located in the cationic position of the zeolite. They also observed displacement of –OH groups around 3610 cm^{-1} in conjunction with the 2133 cm^{-1} band growth to further confirm the location of NO^+. A recent work on NO adsorption onto Cu-CHA by Szanyi et al. [24] has assigned this band to NO^+ paired with Cu^+ ions formed by reduction of Cu^{2+} sites upon interaction with NO^+ and located in cationic position of the zeolite structure. In our DRIFTS experiments, the 2140 cm^{-1} band associated with NO^+ is formed in considerable amounts in the cases of NO_2 adsorption, NO adsorption on the pre-oxidized catalyst and $NO + O_2$ adsorption on the pre-reduced catalyst, whereas the 2140 cm^{-1} peak has an almost negligible intensity in the case of NO adsorption on a pre-reduced catalyst. Also, no perturbation of the 3600–3700 cm^{-1} spectral region is observed. Accordingly, we assign this band to NO^+ species formed upon interaction of NO with Cu sites in an oxidized state, Cu^{2+}. The minor NO^+ formation upon NO adsorption on the pre-reduced Cu-CHA sample can be likely ascribed to an incomplete efficiency of the reducing pre-treatment.

As seen in Fig. 1b for NO_2 adsorption and in Fig. 2 for NO_2 adsorption and NO adsorption on the pre-oxidized catalyst, a shoulder at 2190 cm^{-1} is visible on the NO^+ peak. The same shoulder on the 2140 cm^{-1} peak is reported by Szanyi et al. [25] when feeding NO_2.

Table 1
IR bands detected during NO_x adsorption experiments and their assignments.

IR band (cm^{-1})	Assignment
1570, 1590	Bidentate nitrates
1620	Bridging nitrates
2140	NO^+ formed upon interaction with Cu^{2+}
2190	NO^+NO_2 adducts

The formation of a band at 2185 cm^{-1} under NO_2 adsorption on H-ZSM-5 was pointed out also in [21], where an isosbestic point between the 2133 and 2185 cm^{-1} peaks was also observed, indicating a correlation between the two species. Those bands have been more recently attributed to the formation of NO^+NO_2 adducts in the presence of excess NO_2 in the gas phase [25]. This assignment could explain why in our case the 2190 cm^{-1} band was detected only for NO_2 adsorption and appeared after some time (it is present in Fig. 1b in the 5 min spectrum but not in the previous spectra). In fact, in the case of $NO + O_2$ adsorption, gas-phase NO_2 can hardly be formed via NO oxidation at the considered temperature [12], so that the NO^+NO_2 adduct is not expected in significant amounts.

The 2190 cm^{-1} shoulder has been observed also in the case of NO adsorption on the pre-oxidized catalyst, however, when the presence of gas phase NO_2 is equally unlikely. An alternative interpretation relies on the possible existence of two cationic positions in the zeolite, as pointed out by Peden et al. in recent work [26]: they observed the existence of two distinct Cu^{2+} species in Cu-SSZ-13 characterized by a different reducibility, their distribution depending on the Cu loading. The first Cu ions would be located in the six-membered rings of the zeolite structure, as also proposed by Lobo et al. [27] by Rietveld refinement of XRD measurements, while the second Cu species is assumed to occupy cationic positions in the larger cages of the zeolite structure and is more easily reduced. They also report FTIR data for NO adsorption at room temperature showing a shoulder on the peaks corresponding to NO adsorption on both Cu^+ and Cu^{2+}, assigned to NO adsorbed on Cu sites sitting in the larger cage, growing in intensity as the Cu exchange level increased. Based on all these observations, one could propose a tentative assignment of the 2140 cm^{-1} feature to NO^+ formed in the six-membered ring, while the 2190 cm^{-1} band could be attributed to NO^+ sitting in the larger cages of the CHA structure. Such assignments, however, do not explain why the 2190 cm^{-1} feature is more intense during NO_2 adsorption and appears only after a certain amount of time (Fig. 1b). Considering also the small magnitude of the 2190 cm^{-1} band, it is not possible to establish a conclusive interpretation of the identity of the 2190 cm^{-1} feature detected in our experiments; this, however, does not affect the main conclusions of the present DRIFTS investigation. While the assignment to NO^+NO_2 adducts appears more in line with our experimental results, in the following discussions both peaks in the 2100–2250 cm^{-1} region will be generally regarded as related to NO^+.

A summary of the observed IR bands with their proposed assignments is provided in Table 1.

It is worth mentioning that our data for NO adsorption do not reveal any bands associated with nitrosyls, which were reported instead at 1810 cm^{-1} in similar in-situ DRIFTS studies performed however at 300 K [24,25]. The absence of such species in our spectra is likely due to our significantly higher NO adsorption temperature.

Since the NO_x adsorption spectra compared under different reacting conditions do not point out great differences in the ad-species formed on the catalyst surface besides peak intensities and the presence of the 2190 cm^{-1} shoulder, the role of NO^+ in NO oxidation and the mechanism of nitrates formation are not completely clear at this stage. Then, in order to identify the key players in the NO oxidation mechanism, additional DRIFTS experiments have been

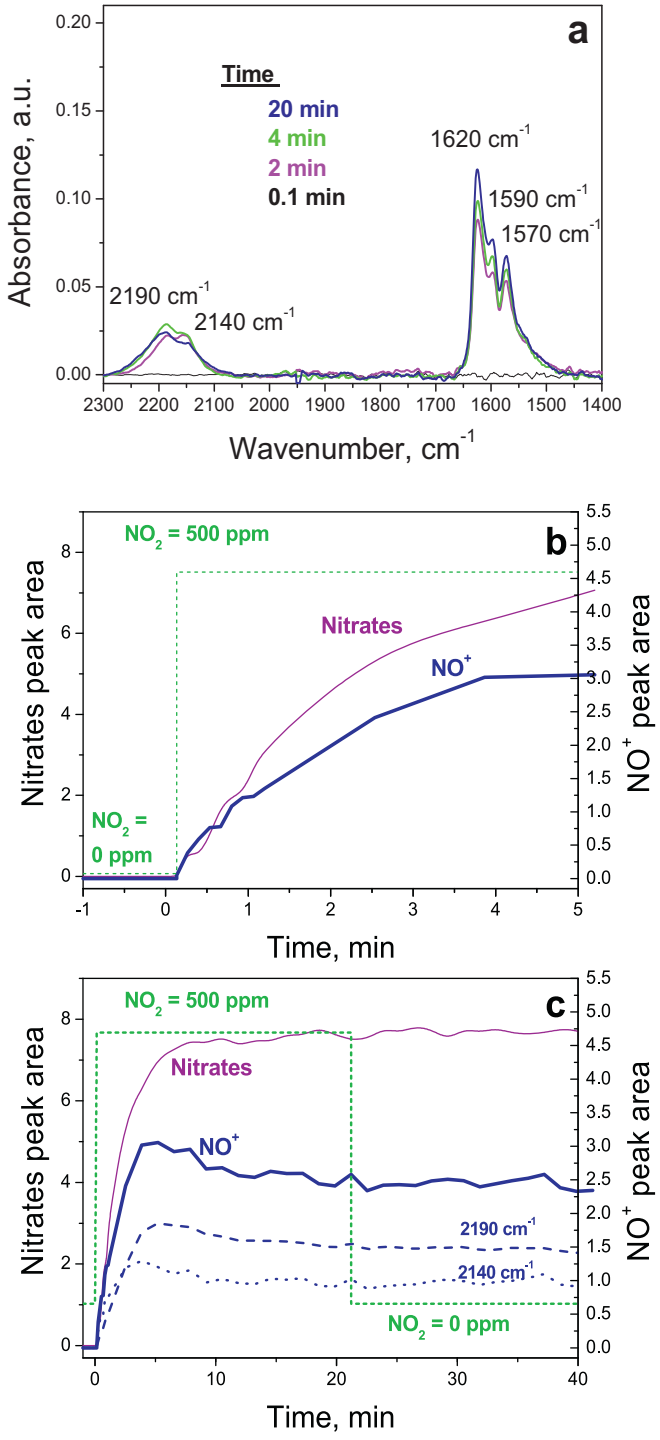

Fig. 3. NO_2 adsorption at 120 °C on pre-oxidized catalyst: (a) selected DRIFT spectra; (b) peak area dynamics during the first 5 min of the experiment; (c) peak area dynamics during the full NO_2 adsorption experiment.

carried out at 120 °C to perform a time resolved analysis of the observed ad-species.

3.2. Peak area dynamics upon NO_x adsorption

3.2.1. NO_2 adsorption dynamics

A series of DRIFTS spectra was collected at 120 °C during NO_2 adsorption experiments in order to monitor the dynamics of surface species formation. Selected spectra are shown in Fig. 3a immediately after NO_2 feed (500 ppm) and after 2, 4 and 20 min. In addition, the peak area profiles for nitrates and NO^+ are shown in Fig. 3b and c, in which the stepped NO_2 feed is displayed as well. The initial 5 min are magnified in Fig. 3b. Integration of the peak areas corresponding to nitrates was evaluated considering all the three features in the 1400–1700 cm^{-1} region. Similarly, the NO^+ peak area is calculated integrating over the entire 2000–2300 cm^{-1} region. No deconvolution of the peaks was carried out and the peak areas referring to the 2140 and 2190 cm^{-1} features were calculated by integrating the 2000–2170 and the 2170–2300 cm^{-1} spectral region, respectively, the NO^+ area being therefore the sum of the 2140 and 2190 cm^{-1} contributions.

The spectral features at 120 °C are the same as the peaks present at 150 °C (Fig. 1). As soon as NO_2 is fed to the reactor cell, trace levels of both NO^+ and nitrates are observed. As time increases, both peaks grow in intensity, suggesting that those two species are formed on the surface at the same time. The nitrate bands, however, continue to grow monotonically with time approaching a steady state, whereas the bands corresponding to NO^+ reach a maximum intensity after about 2 min and then slowly decrease with time. The decline in the NO^+ band signal parallels the increase of the nitrates bands, thus suggesting conversion of NO^+ to nitrates. Note that different extinction coefficients of the involved species may account for the differences in the peak areas, which do not quantitatively correlate 1:1. Moreover, it should also be considered that a fraction of NO^+ intermediates could be in equilibrium with nitrite species that are not visible in our IR measurements as their bands are obscured by the features of the zeolite framework.

The peak area dynamics shown in Fig. 3b, which reports the first 5 min of the experiment, highlight more clearly the previous observations: when NO_2 is present in the gas phase, NO^+ and nitrates are formed simultaneously on the catalyst surface. Moreover, NO^+ decreases beyond 2 min, while nitrates are in the final approach to steady-state surface concentration. Such a behavior suggests that NO^+ might be an intermediate in the conversion of NO_2 to nitrates, being formed initially via NO_2 disproportionation—heterolytic chemisorption and then rapidly oxidized by NO_2 in the process of nitrates formation [7,8]. Moreover, NO^+ is relatively stable at 120 °C, since it is still present in significant amounts after nitrates reach their steady-state concentration, and its peak area remains constant even after NO_2 shut off (Fig. 3c). Similar NO_2 adsorption experiments at a higher temperature (150 °C) showed, however, partial disappearance of NO^+ after NO_2 shut-off, while nitrates remained stable, as illustrated in Fig. 4. The comparison of Figs. 3 and 4 suggests that the NO^+ stability decreases with increasing temperature.

Notably, an FTIR study of NO_2 adsorption onto Fe-ZSM-5 showed a similar evolution of NO^+ and nitrates species during exposure of the catalyst to NO_2 at low temperature, but only nitrates were left at steady-state after NO_2 shut-off [8]. The different behavior of NO^+ ad-species observed in this work and by Ruggeri et al. [8] are in line with the greater stability of nitrates and nitrites on Cu-zeolites as compared to Fe-zeolites [28].

3.2.2. $NO + O_2$ adsorption dynamics

The same experiment was replicated at 120 °C on a pre-oxidized catalyst (Fig. 5), feeding simultaneously NO and O_2: oxygen flow was kept constant during the experiment, whereas NO (500 ppm) was fed for 30 min and then shut off. As apparent in the spectra in Fig. 5a (immediately after NO feed and after 3, 15, 30 and 40 min), both NO^+ and nitrates are already present after 3 min of NO feed. However, the two bands grow with different rates: the NO^+ band is relatively constant after 3 min, while the nitrates bands continue to grow. In addition, on comparing the evolution of the peak area

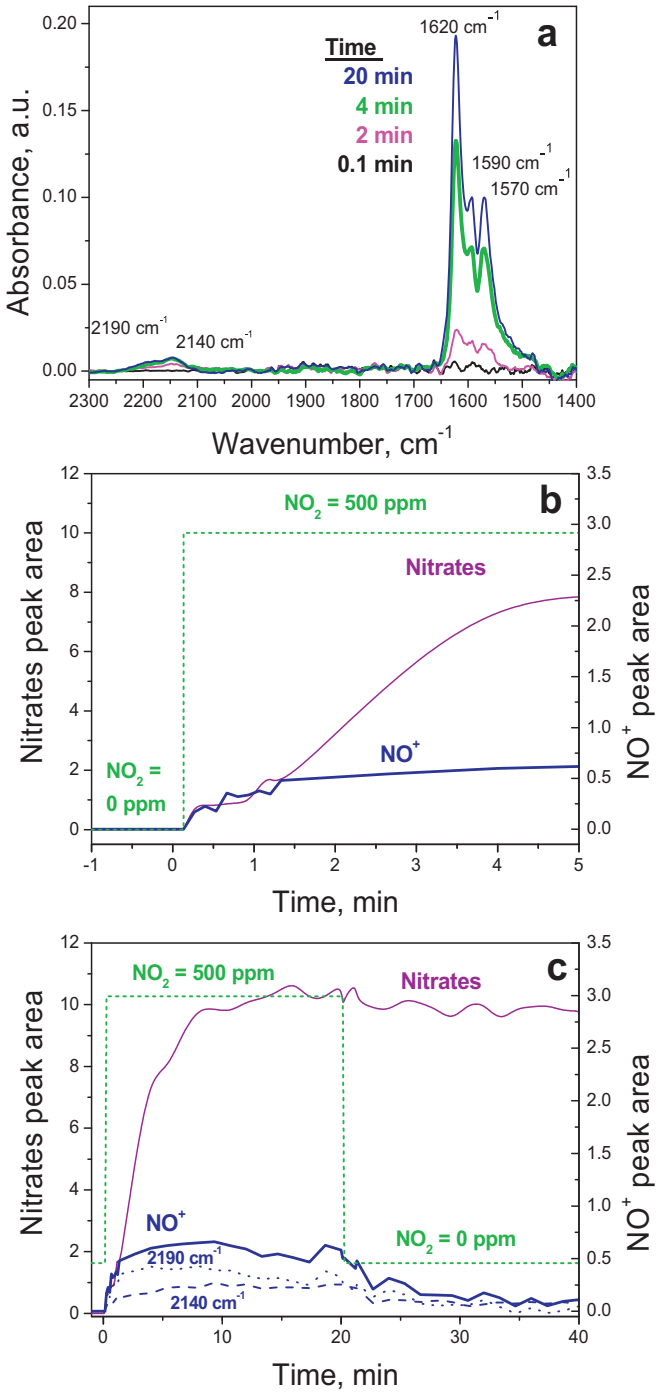

Fig. 4. NO_2 adsorption at 150 °C on pre-reduced catalyst: (a) selected DRIFT spectra; (b) peak area dynamics during the first 5 min of the experiment; (c) peak area dynamics during the full NO_2 adsorption experiment.

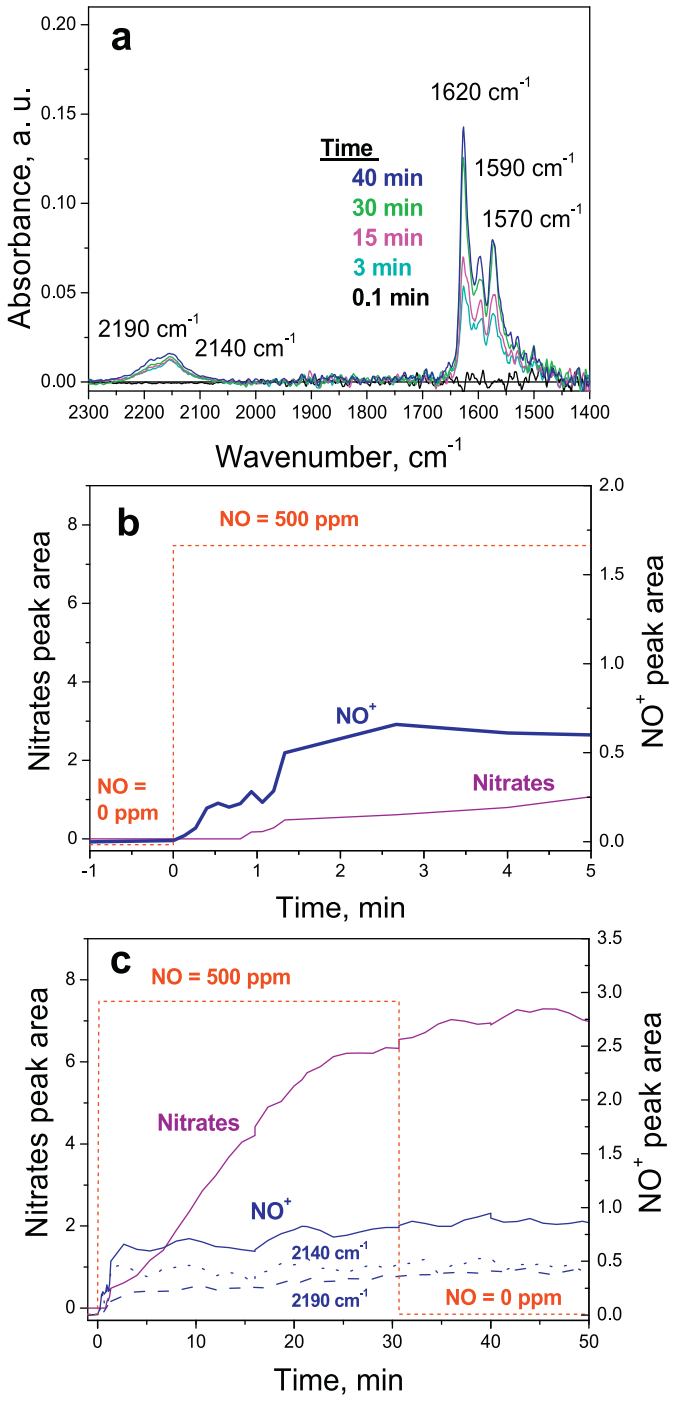

Fig. 5. $NO + O_2$ adsorption at 120 °C on pre-oxidized catalyst: (a) DRIFT spectra; (b) peak area dynamics during the first 5 min of the experiment; (c) peak area dynamics during the full $NO + O_2$ adsorption experiment.

profiles displayed in Fig. 5b and c, it is apparent that the 2140 cm^{-1} band increases as soon as NO is added to the 8% O_2 in Ar gas feed mixture. Nitrates, on the contrary, are formed on the catalyst surface with a small delay and at a different rate. In fact, in the first 5 min of NO adsorption, the NO^+ peak area grows rapidly, whereas nitrates are formed slowly (Fig. 5b).

Notably, comparison of Fig. 5 with Fig. 3 reveals the differ-ent temporal evolution of the same ad-species (NO^+ and nitrates) observed when the Cu-zeolite catalyst is exposed to $NO + O_2$ (Fig. 5) rather than to NO_2 (Fig. 3). It is clearly apparent that during the oxidative activation of NO the formation of NO^+ precedes the formation of nitrates, contrary to the simultaneous appearance of both species during NO_2 adsorption. Accordingly, these data: (i) rule out that the initial activation of NO leads directly to gaseous NO_2, since in this case the expected surface species evolution should be the same as in NO_2 adsorption; (ii) suggest a role of intermediate for NO^+ (and related species, like nitrites) in the NO oxidation process. The importance of NO^+ as an intermediate in the SCR chemistry has also been recently addressed by Szanyi et al. [24], who identified NO^+ as an intermediate in the Standard SCR reaction over Cu-SSZ-13.

It is worth emphasizing that the decrease in the NO^+ peak area and the corresponding increase in the nitrates peak area are not expected to quantitatively correlate 1:1, due to the different molar extinction coefficients of NO^+ and nitrates. In this respect, it should also be considered that a possibly considerable fraction of the surface intermediates (e.g. nitrites in equilibrium with NO^+ species, see step R.2) may not be visible to IR as their bands are obscured by the features of the zeolite framework.

The same $NO + O_2$ adsorption experiment (here not shown) was replicated on a pre-reduced catalyst and the results revealed the same qualitative behavior described for the pre-oxidized catalyst. Thus, an oxidizing or reducing pre-treatment did not have any effect on $NO + O_2$ adsorption as regards both surface species formation and peak area dynamics.

3.2.3. *Dynamics of NO adsorption on pre-oxidized catalyst*

Fig. 6a shows the spectra collected during NO adsorption with no O_2 co-feed at 120 °C on a pre-oxidized Cu-CHA sample immediately after starting the NO feed, and after 3, 15, 30 and 40 min of NO exposure. After 3 min, only NO^+ is present on the catalyst surface, while nitrates are formed at later times, even without oxygen in the gas phase. The peak area dynamics displayed in Fig. 6b and c are similar to the case of $NO + O_2$ adsorption both on the pre-reduced and on the pre-oxidized catalyst, and differ from the case of NO_2 adsorption. In fact, the areas corresponding to the two species of interest, namely nitrates and NO^+, do not grow simultaneously. Indeed, as soon as NO is fed to the catalyst sample, NO^+ species are formed first, whereas nitrates are formed after a delay, beginning to grow only after 5 min. This evidence clearly suggests that the two species are formed in sequence: $NO^+ \rightarrow$ nitrates, like in the case of the $NO + O_2$ experiment in Fig. 5 and differently from the simultaneous evolution noted during NO_2 adsorption in Figs. 3 and 4. Moreover, the experiment proves the red-ox nature of NO oxidation to surface NO^+ and nitrates: since there is no oxygen in the gas phase, NO must be reacting with oxygen from the catalyst.

3.2.4. *Dynamics of NO adsorption on pre-reduced catalyst*

NO adsorption on a pre-reduced catalyst sample was also performed without feeding oxygen: related DRIFTS spectra collected before NO feed and after 0.1, 4 and 10 min are shown in Fig. 7a. As NO is fed to the Cu-CHA sample, no interaction with the sur-face is observed for the first few minutes. Then, a little NO^+ is slowly formed on the surface. This can be probably ascribed to the presence of a few oxidized Cu sites not fully reduced during the sample pre-treatment with NH_3. Evidence of incomplete reduction of the catalyst with formation of small amounts of NO^+ on a pre-reduced Cu-CHA is also reported by Szanyi et al. [25]. It is worth emphasizing, however, that no nitrates are formed on the catalyst when oxygen is absent from both the gas phase and from the catalyst surface. Only when O_2 is present (see Figs. 5 and 6) NO^+ is detected in large amounts on the catalyst surface and the nitrates peak area grows. This experiment, together with the NO adsorption runs described earlier and reported in Figs. 5 and 6, confirms the red-ox nature of the entire process of NO oxidation to surface NO^+ and nitrates.

3.3. *Water effect on NO_2 adsorption*

All the experiments discussed so far were carried out in the absence of water. However, in realistic SCR conditions water is always present, being a significant part of the engine exhaust. For this reason, the effect of water on the catalyst surface species has also been investigated. NO_2 adsorption was performed while continuously feeding 1% of water to the reactor cell. Fig. 8 compares

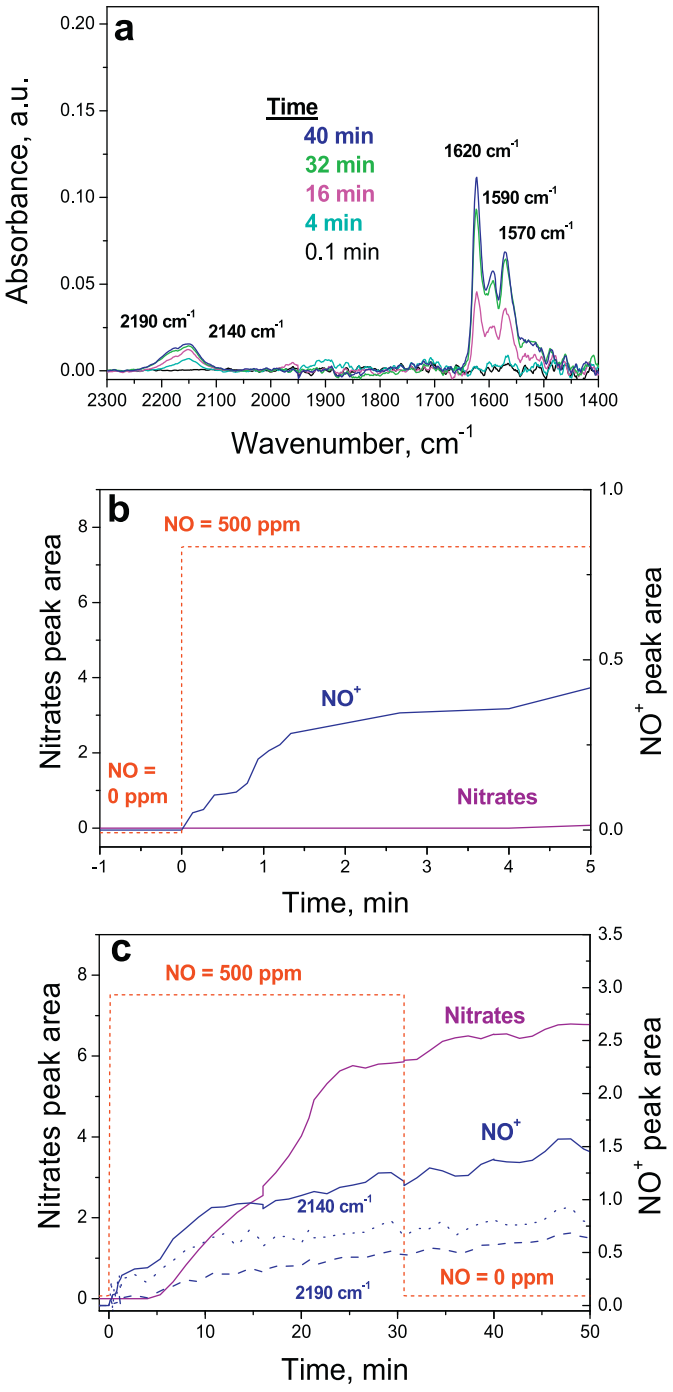

Fig. 6. NO adsorption at 120 °C on pre-oxidized catalyst: (a) selected DRIFT spectra; (b) peak area dynamics during the first 5 min of the experiment; (c) peak area dynamics during the full NO adsorption experiment.

DRIFTS spectra collected at 150 °C after 20 min of NO_2 adsorption both in the absence and presence of water on a pre-reduced catalyst. Fig. 8 shows that no NO^+ was detected with water present. Moreover, nitrates were present but to a much less extent. This suggests that water adversely affects the NO oxidation process, hindering the formation of NO^+ and of related intermediates [22], and thus inhibiting nitrates formation on the catalyst surface. Indeed, it has been extensively reported in the literature that water has a strong inhibiting effect on NO oxidation to NO_2 [12] and negatively affects nitrates formation [29].

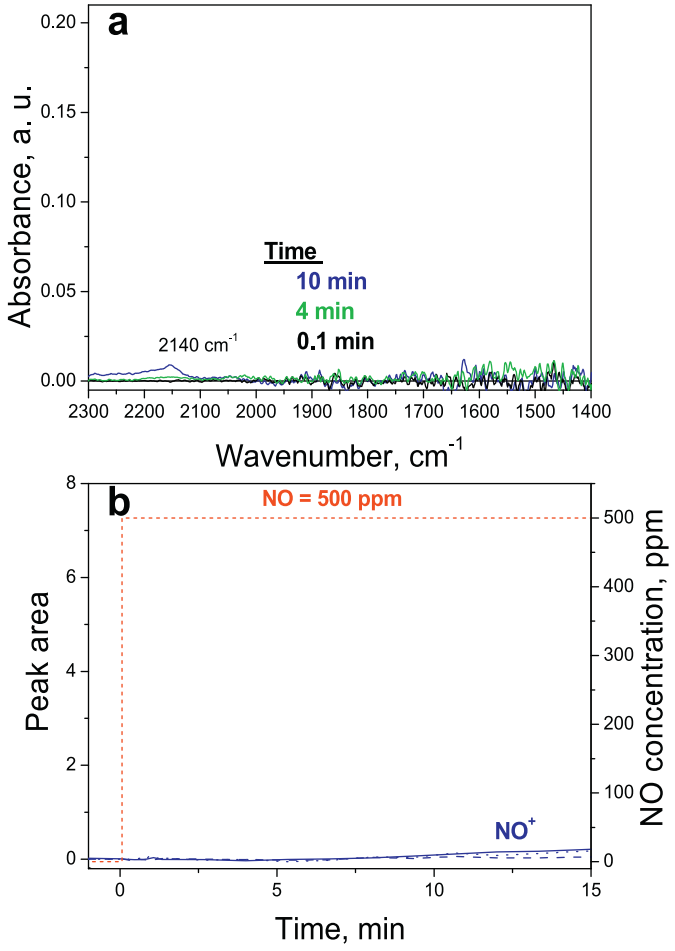

Fig. 7. NO adsorption at 120 °C on pre-reduced catalyst (no O_2 feed): (a) selected DRIFT spectra; (b) peak area dynamics during NO adsorption on a pre-reduced catalyst.

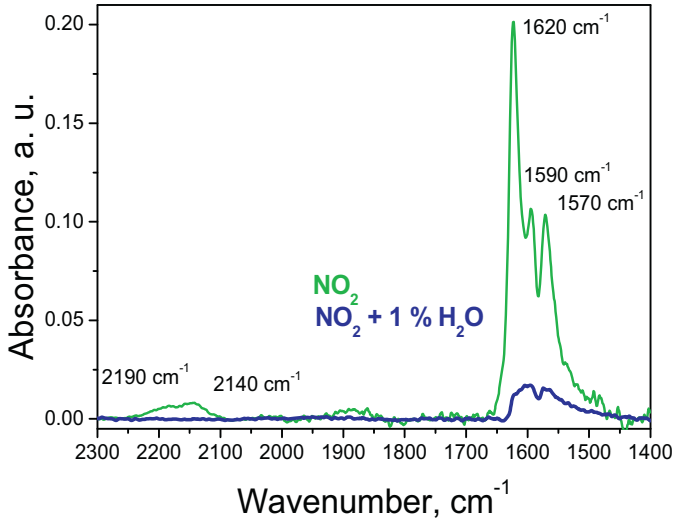

Fig. 8. Selected DRIFT spectra for NO_2 adsorption on pre-reduced catalyst at $T = 150$ °C after 20 min: H_2O effect.

3.4. Proposed reaction mechanism for NO oxidation

3.4.1. Active sites

Based on the in-situ DRIFTS results reported above, a mechanistic proposal for NO oxidation over Cu-CHA should account for the following features:

1) NO^+ and nitrates are the primary surface species formed during NO oxidation.
2) The process of NO oxidation and nitrates formation has a redox nature: it proceeds not only in the presence of gas-phase oxygen, but oxygen reacts directly from the surface of the catalyst; moreover, the reaction does not proceed on a pre-reduced catalyst.
3) Different dynamics prevail depending on the species present in the gas phase (NO_2, $NO + O_2$, NO on a pre-oxidized catalyst). In particular, during NO adsorption/oxidation nitrates are formed consecutively to NO^+, whereas simultaneous formation of NO^+ and nitrates occurs during NO_2 adsorption.
4) In the presence of water, only small amounts of nitrates are formed.

It is worth pointing out that, in our experiments, different Cu oxidation states, namely Cu^{2+} for the pre-oxidized sample and Cu^+ for the pre-reduced catalyst, were likely induced by different catalyst pre-treatments. Preliminary considerations on the nature of the Cu sites and their configuration and coordination in the zeolite structure are necessary for the discussion of the NO oxidation mechanism. Indeed, the species detected during NO_x adsorption are reported to be associated with Cu^{2+} placed in the cationic position of the zeolite structure, both in the case of NO^+ and of nitrates. In fact, only traces of NO^+ were formed on the pre-reduced catalyst, on which Cu could be present as Cu^+. The amount of NO^+ detected in these experiments was negligible compared to that formed on the pre-oxidized sample and appeared after a substantial delay. As a consequence, it can be inferred that no NO^+ is formed when the oxidation state of copper is +1. Indeed, the presence of Cu^{2+} in the zeolite framework balances two negative charges in the aluminosilicate zeolite framework: the same charge compensation can be provided by a NO^+–Cu^+ pair formed upon donation of an electron to Cu^{2+} [25]. This proposal is supported by McEwen et al. [30], who published X-ray adsorption data and DFT calculations for characterization of the Cu oxidation state in operando conditions for a Cu-CHA catalyst. This study concluded that the average oxidation state of Cu in presence of NO_2 (i.e. during both NO oxidation and Fast SCR experiments) is +2, whereas it is +1 for standard SCR conditions, when NO_2 is not present. Cu^0 was not, in any case, a plausible oxidation state for Cu. This implies that an oxidized catalyst is needed for NO oxidation to proceed and brings us to the conclusion that NO interacts with Cu^{2+} to form NO^+ as an intermediate species in the NO oxidation process. NO^+ is, of course, an oxidized intermediate: the formal N oxidation state goes in fact from +2 to +3 in $NO \rightarrow NO^+$.

It has been proposed that in Cu-CHA catalysts, single isolated Cu sites exist coordinated with three oxygen atoms [30–33]. For other zeolites such as Cu-ZSM-5 [34,35], however, the existence of Cu dimers has been reported and proposed as responsible for the activity in the selective catalytic reduction of NO_x by ammonia. More recently, the existence of Cu dimers on Cu-CHA zeolite catalysts has been reported [36,37], too, in the case of highly Cu-loaded samples, like, e.g., commercial NH_3-SCR catalysts similar to the one used in the present investigation. A very recent experimental and computational kinetic study [38] has provided clear evidence, based both on in-situ XANES and on DFT calculations, that only Cu_xO_y sites ($x \geq 2$) contribute linearly to the NO oxidation activity over Cu-SSZ-13, whereas isolated monomeric Cu ions

cannot accommodate adsorption and dissociation of O_2 necessary to catalyze NO oxidation. In this respect, it may be also worth noticing that formation of NO^+ involves reduction of one Cu^{2+} to Cu^+; once NO^+ has been formed, however, one more oxidized Cu^{2+} site is needed in order to complete the NO oxidation process, bringing the NO^+ intermediate (+3) to NO_2 (+4). In other words, the two-step oxidation of NO to NO_2 requires an overall increment of +2 in the formal oxidation state of nitrogen: this suggests that it may proceed more effectively over dimeric Cu-sites.

In line with the literature evidence above, we identify Cu dimers as the most likely candidates to be the active sites for NO oxidation to NO_2 in our experimental conditions. Notably, this does not necessarily imply that the same sites are also responsible for the NH_3-SCR activity.

3.4.2. Mechanism of NO oxidation to NO_2

In light of the previous considerations, we assume small copper clusters, in the form of Cu dimers, as the active sites for NO oxidation. The first step (R.1) in the redox mechanism of NO oxidation can thus be written as:

$$Z-O-[Cu^{II}OCu^{II}]^{II}-O-Z+NO \leftrightarrow Z-(O-Cu^{II}O)^{-}NO^{+}+Cu^{I}-O-Z \quad \text{(R.1)}$$

Step (R.1) proceeds on a copper dimer: on one Cu site, a nitrosonium ion is formed, whereas the other Cu is reduced to Cu^I. This reaction implies the formation of an oxidized species: $Cu^{II}O^{-}NO^{+}$ can be identified as the precursor of a nitrite, in which the nitrogen atom is in a +3 formal oxidation state (R.2):

$$Z-(O-Cu^{II}O)^{-}NO^{+} \leftrightarrow Z-O-Cu^{II}-NO_2 \quad \text{(R.2)}$$

This species is detected as "NO^+", namely the species corresponding to the 2140 cm^{-1} band, in our DRIFTS experiments. On the other hand, no nitrites were detected during the same experiments, perhaps due to the highly reactive and unstable nature of such species. Moreover, characteristic nitrites IR bands would be masked by the IR absorbance features of the zeolite (wavenumber < 1300 cm^{-1}) [8,39]. Spectral inspection for the presence of a band around 2444 cm^{-1}, corresponding to nitrites combination/overtone modes, as reported in [20], did not give any definitive conclusion. Indeed, if visible, we expect that the contributions both of nitrites (at 1220 cm^{-1}) and of the corresponding combination modes would be very small.

Proceeding from step (R.1), NO_2 is then formed directly from decomposition of the nitrite-like species according to (R.3), which leads to the formation of a second Cu in a reduced state. This is regarded as the rate determining step of the NO to NO_2 process [8,40]:

$$Z-(O-Cu^{II}O)^{-}NO^{+} \leftrightarrow NO_2+Cu^{I}-O-Z \quad \text{(R.3)}$$

Finally, in order to close the redox cycle, the Cu sites have to be reoxidized by oxygen:

$$2Cu^{I}-O-Z+\frac{1}{2}O_2 \rightarrow Z-O-[Cu^{II}OCu^{II}]^{II}-O-Z \quad \text{(R.4)}$$

Reaction (R.4) is of course not an elementary step, possibly implying mobility of surface oxygen atoms.

The sum of steps (1)–(3) gives the overall NO oxidation reaction (4):

$$NO+\frac{1}{2}O_2 \rightarrow NO_2 \quad \text{(R.5)}$$

The mechanism discussed above is written in the absence of water and accounts for the experimental observations collected during this study, namely:

1) The pre-oxidized catalyst is active in NO^+ and nitrates formation, whereas no species are formed on the pre-reduced catalyst;
2) NO^+, with a formal N oxidation state of +3, behaves as an intermediate in NO (+2) oxidation to NO_2 (+4);
3) The red-ox nature of NO oxidation to NO_2 requires an overall change of 2 in the catalyst oxidation state.

The water effect will be discussed in a dedicated section below.

3.4.3. Mechanism of surface nitrates formation

Contrary to what was observed for NO oxidation to NO^+, in the presence of NO_2 nitrates formation proceeds simultaneously with NO^+ formation. As extensively reported in literature, the related mechanism likely implies disproportionation of NO_2 to nitrites/nitrates, and subsequent oxidation of nitrites to nitrates, accompanied by NO evolution, according to the following reactions [41]:

$$Z-O-[Cu^{II}OCu^{II}]^{II}-O-Z+2NO_2 \leftrightarrow Z-(O-Cu^{II}O)^{-}NO^{+}+Z-O-Cu^{II}-NO_3 \quad \text{(R.6)}$$

$$Z-(O-Cu^{II}O)^{-}NO^{+}+NO_2 \leftrightarrow Z-O-Cu^{II}-NO_3+NO \quad \text{(R.7)}$$

wherein a NO^+/nitrite species is formed in addition to a nitrate by dimerization and heterolytic adsorption of NO_2 and then reacts with gaseous NO_2 to form NO and one more nitrate. These reactions can explain the efficient nitrate formation observed in Fig. 3 for NO_2 adsorption on a pre-oxidized sample. It should be emphasized that, contrary to the case of NO oxidation, nitrate formation from NO_2 does not require a change in the catalyst oxidation state, i.e. it remains as Cu^{2+}.

In the case of a pre-reduced catalyst, it was observed that no NO^+ could be formed on the surface of the catalyst when exposed to NO only. Without O_2, in fact, NO_2 is needed to re-oxidize the catalyst to form NO^+:

$$Z-O-Cu^{I}+NO_2 \leftrightarrow Z-(O-Cu^{II}O)^{-}NO^{+} \quad \text{(R.8)}$$

and then NO^+ reacts with additional NO_2 to form nitrates and NO similarly to what reported for the oxidized sample (R.7). Notably, the red-ox step (R.8), involving oxidation of a reduced Cu site, is nothing but the reverse of (R.3).

Our results show that nitrates can be formed also from NO adsorption, when feeding either NO + O_2 or NO only over a pre-oxidized catalyst (Figs. 5 and 6, respectively), the differences relative to NO_2 exposure being that (i) NO^+ and nitrates are now formed in a stepwise sequence and (ii) oxygen is required, either from the gas phase or from the catalyst surface. These elements suggest that nitrates formation on the catalyst may result from NO_2 evolution in the gas phase according to the same mechanism summarized by steps (R.6)–(R.7). Notably, this hypothesis is not ruled out by the experiments with gas phase monitoring (not shown here), wherein no NO_2 was detected, because even small traces of NO_2 could still disproportionate and form nitrates.

Buildup of stable surface nitrates blocking the active Cu-sites explains the well-known significant NO_2 inhibition of the NO oxidation to NO_2 noted experimentally over metal-promoted zeolite catalysts [9].

3.4.4. NO oxidation to NO_2 and nitrates formation in the presence of water

Water likely has an effect on the configuration of Cu sites within the zeolite structure [36]. In particular, water would be responsible for the following reaction:

$$Z-O-[Cu^{II}OCu^{II}]^{II}-O-Z+H_2O \leftrightarrow 2Z-(O-Cu^{II}O)^{-}H^{+} \quad \text{(R.9)}$$

Evidence of CuOH groups formed upon dissociative adsorption of H_2O has been indeed obtained in our DRIFT experiments (band at 3670 cm^{-1}), based on the assignment recently proposed by Giordanino et al. [42]. The formation of CuOH species as a result of the hydration of Cu dimers is also reported in [36,43]. On the other hand, molecular adsorption of water and formation of $[Cu(H2O)_6]^{2+}$ complexes is reported to result from hydration of isolated Cu species [36,38] which, according to [38], do not contribute significantly to the rate of NO oxidation.

Notably, (R.9) results in the disruption of the Cu dimers, i.e. the sites responsible for the NO oxidation process according to our proposal. In addition, it can be speculated that CuOH sites are inactive (or less active) in the NO oxidation to NO_2, consistently with what proposed for isolated Cu sites [38]. Furthermore, in the presence of water, NO^+ can be hydrolyzed, in line with what has been reported for Fe-zeolites [7,12,24], according to

$$Z-(O-Cu^{II}O)^{-}NO^{+}+H_2O \leftrightarrow Z-(O-Cu^{II}O)^{-}H^{+}+HONO \quad \text{(R.10)}$$

In fact, the DRIFTS results for NO_2 adsorption experiments in wet conditions, shown in Fig. 8, confirm that no NO^+ is detected when water is present. Notably, both the breakage of the active dimeric Cu-sites, (R.9), and the (R.10) equilibrium are consistent with the experimentally observed strong H_2O inhibition of the NO oxidation to NO_2 [12].

When H_2O is present, however, nitrates are still formed in small quantities upon NO_2 adsorption, so a mechanism accounting for the formation of nitrates in wet conditions has to be considered, too. In particular, nitrates are formed both on pre-oxidized and on pre-reduced catalysts [41].

A mechanism of nitrates formation on CuOH sites can be written in analogy with the mechanism reported in the literature for Fe-zeolites [8], e. g.

$$2NO_2+Z-(O-Cu^{II}O)^{-}H^{+} \leftrightarrow Z-(O-Cu^{II}O^{-})NO^{+}+HNO_3 \quad \text{(R.11)}$$

$$HNO_3+Z-(O-Cu^{II}O)^{-}H^{+} \leftrightarrow Z-O-Cu^{II}-NO_3+H_2O \quad \text{(R.12)}$$

$$NO_2+Z-(O-Cu^{II}O^{-})NO^{+} \leftrightarrow Z-O-Cu^{II}-NO_3+NO \quad \text{(R.13)}$$

This process proceeds via gaseous HNO_3 (R.11), which forms nitrates interacting with a Cu site (R.12). The formation of nitrates, however, is influenced by the water concentration: high concentrations of water would negatively affect the (R.12) equilibrium, thus reducing the concentration of surface nitrates, as experimentally observed.

3.5. Catalytic activity tests and kinetic effects of O_2, H_2O and NO_2 on NO oxidation

The NO oxidation and Standard SCR activity of the Cu-CHA catalyst employed in the present in-situ DRIFTS study have been investigated under dry conditions. Steady-state data obtained from the bench reactor runs are plotted in Fig. 9 in terms of NO average consumption rate ($mol_{NO}/(g_{cat}{}^{*}s)$). A Standard SCR activity was apparent already at 150 °C and grows with increasing temperature: an average rate of approximately 1.3×10^{-3} $mol_{NO}/(g_{cat}\,s)$ was approached at 250 °C. On the contrary, the NO oxidation activity was very low: negligible activity was noted at 150 °C, and an average rate of only 1.3×10^{-4} $mol_{NO}/(g_{cat}\,s)$ was achieved at 350 °C. Notice that our data show a difference of at least one order of magnitude in the measured average rates of NO consumption for the two reactions. These results are typical of state-of-the-art Cu-CHA commercial SCR catalysts. Particularly, average rate values calculated from data available in literature and collected at the same temperatures are in the order of 10^{-3} $mol_{NO}/(g_{cat}\,s)$ and 2.8×10^{-4} $mol_{NO}/(g_{cat}\,s)$ for standard SCR [43] and NO oxidation, respectively [9], in line with results herein reported. This confirms

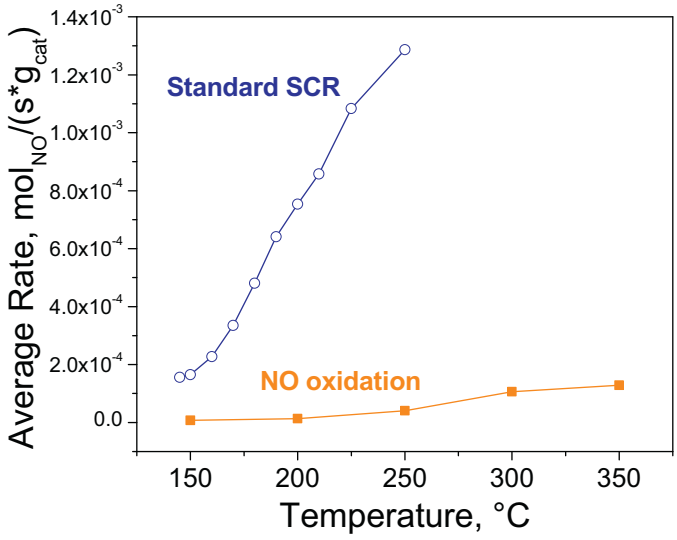

Fig. 9. Integral average rates for NO oxidation and Standard SCR reaction. Experimental conditions: NO oxidation, GHSV = 30000 h^{-1} (Q = 4985 Ncc/min; W_{cat} = 3.98 g), NO = 500 ppm, O_2 = 8%, H_2O = 0%; Standard SCR, GHSV = 90000 h^{-1} (Q = 14955 Ncc/min; W_{cat} = 3.98 g), NO = 500 ppm, NH_3 = 500 ppm, O_2 = 8%, H_2O = 0%.

that the NO oxidation activity is very poor compared to Standard SCR activity over Cu-promoted zeolites [9,12,28].

Focusing on NO oxidation, the kinetic effects of water, oxygen and NO_2 concentration have been investigated with the main purpose of verifying their coherence with our mechanistic proposal. Fig. 10a compares NO average consumption rates obtained varying the oxygen feed concentration and adding water to the feed gas stream. Lowering the oxygen feed concentration from 8 to 2% (v/v) resulted in a decreased NO oxidation activity, in accordance with literature reports [9]. Furthermore, switching from dry to wet conditions at constant 8% O_2 essentially suppressed the NO oxidation activity, again in line with previous reports [12].

Fig. 10b shows the NO oxidation results obtained for an experiment in which the total NO_x feed concentration was kept constant, while the NO_2/NO_x feed ratio was varied from 0 to 0.75 in the presence of 8% O_2 and absence of water: measured NO average consumption rates are plotted as a function of the NO_2/NO_x ratio at different reaction temperatures. As the NO_2 content in the feed increased, NO average consumption rates decreased at all temperatures, revealing a strong inhibiting effect of NO_2 on the NO oxidation rate. Such observations are in line with Metkar et al. [9].

The experimental results in Figs. 9 and 10 are strong evidence that NO oxidation to NO_2 does not represent the rate determining step of the Standard SCR reaction, as has been proposed elsewhere [12]. On the contrary, our mechanistic proposal well explains the experimental evidence in Fig. 10. In particular, the inhibiting effect of water is explained by formation of less reactive Cu(OH) isolated sites [36] according to step (R.9), and by the equilibrium between HONO formed upon H_2O interaction with surface NO^+ and NO^+ itself, expressed by step (R.10): once HONO is formed, in fact, step (R.3) (NO^+ decomposition to NO_2) cannot proceed further to produce gaseous NO_2.

The NO_2 inhibiting effect can be explained by: (i) shift of the equilibrium of (R.3) towards NO^+ due to the presence of gas-phase NO_2; (ii) formation of stable nitrates on the Cu sites, which impedes further proceeding of the NO oxidation reaction. Moreover, the mechanism herein proposed is not in contrast with the identification of nitrites species as key intermediate in the Standard SCR reaction, as recently suggested by Ruggeri et al. [44] for Fe zeolite catalysts.

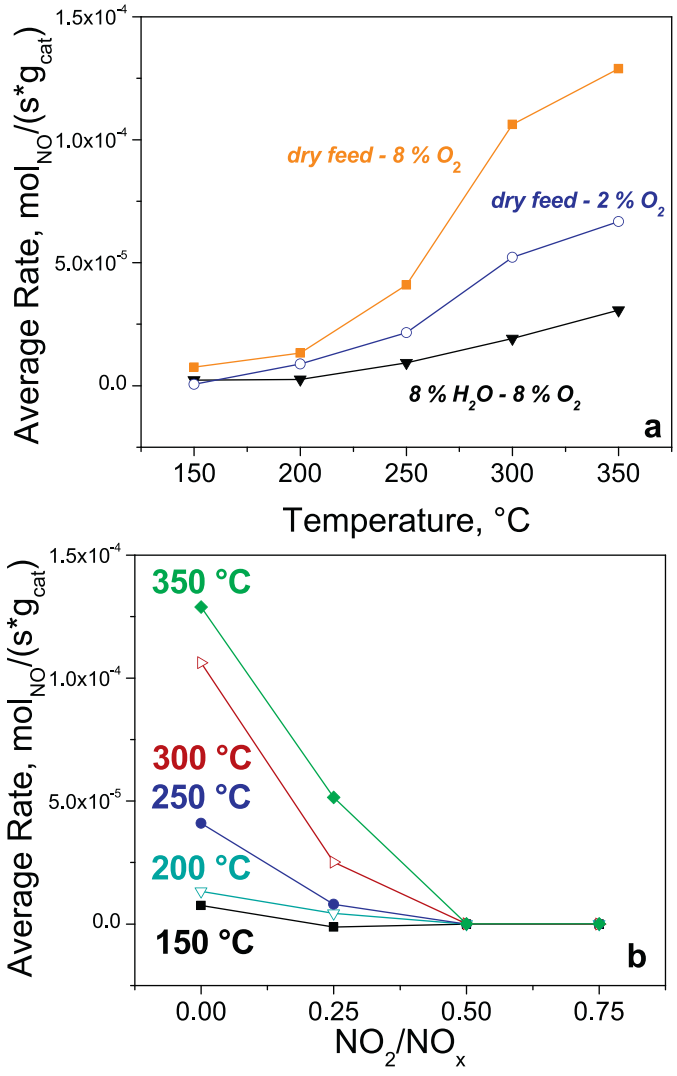

Fig. 10. Integral average rate of NO oxidation. (a) Oxygen and water effects. Experimental conditions: NO oxidation, GHSV = 30000 h^{-1} (Q = 4985 Ncc/min; W_{cat} = 3.98 g), Feed: NO = 500 ppm, O_2 = 2–8%, H_2O = 0–8%. (b) NO_2 effect. Experimental conditions: NO oxidation, GHSV = 30000 h^{-1} (Q = 4985 Ncc/min; W_{cat} = 3.98 g), Feed: NO_x = 500 ppm, NO_2/NO_x = 0–0.75, O_2 = 8%, H_2O = 0%.

4. Conclusions

NO oxidation to NO_2 and its mechanism have been studied over a commercial state-of-the-art Cu-CHA NH_3-SCR catalyst by in-situ DRIFT spectroscopy. Adsorption of NO_2, NO + O_2 and NO on both pre-oxidized and pre-reduced catalyst samples have been analyzed in order to identify the surface species involved in the overall NO oxidation process. Under oxidizing conditions, nitrates on Cu^{2+} were the dominant ad-species on the catalyst surface at steady state after NO_x adsorption for ≈20 min. Formation of nitrates by NO adsorption on the pre-oxidized catalyst did not require gas-phase O_2, as oxygen was supplied directly from the catalyst surface.

Another ad-species besides nitrates was identified as NO^+, nitrosonium ion. NO^+, having a formal N oxidation state of +3, can be considered a nitrite-like species, formed as an intermediate in the stepwise oxidation process from NO (+2) to NO_2 (+4). The observed temporal evolution of the species in fact supports the hypothesis of NO^+ (or related nitrites) as intermediates in NO oxidation: NO^+ appeared before nitrates when NO was fed to the reactor, whereas it appeared simultaneously with the nitrates in NO_2 adsorption runs. This result is of great importance, since it reveals that the formation of the above-mentioned NO^+ species proceeds from either NO + O_2 or NO_2 via two different mechanisms, namely oxidation of NO over Cu^{2+}, which involves Cu reduction to Cu^+, and NO_2 disproportionation–heterolytic chemisorption, which leaves the Cu^{2+} sites in their high oxidation state. Based on recent literature reports, it is also assumed that NO oxidation to NO^+ proceeds on Cu dimers, which are known to be present in commercial Cu-CHA catalysts with high Cu loadings.

The DRIFTS experiments have clearly pointed out the red-ox nature of the NO oxidation to NO_2, since only traces of NO^+ and no nitrates were formed on a pre-reduced catalyst when feeding NO only, without gas-phase oxygen.

The effect of water on the NO oxidative activation was also addressed: no NO^+ species and only trace amounts of nitrates were detected in NO + O_2 adsorption experiments under wet conditions. Such a result is explained considering that water hydrolyzes the Cu dimers, i.e. the active sites in NO oxidation, and also shifts the NO^+/nitrites–HONO equilibrium. Likewise, water also adversely affects nitrates formation via NO_2 disproportionation by acting on the nitrates–HNO_3 equilibrium.

A comprehensive mechanism for NO oxidation to NO_2 and nitrates has been formulated, which is consistent with all of the above-mentioned observations. The proposed mechanism is in accordance with the observed kinetic effects of H_2O, O_2 and NO_2 on the NO oxidation activity of the Cu-CHA catalyst.

DRIFTS measurements similar to those herein reported with the aim to investigate the standard SCR mechanism and related surface species were performed on the same catalyst and will be presented and discussed in a dedicated forthcoming paper.

Acknowledgments

The authors wish to thankfully acknowledge Dr. Jae Soon Choi from the Fuels, Engines, and Environment Emissions Research Center of the Oak Ridge National Laboratory for his valuable contribution to results discussion.

This work is a collaboration between the Laboratory of Catalysis and Catalytic Processes, Dipartimento di Energia, Politecnico di Milano, and Oak Ridge National Laboratory's Fuels, Engines, and Emissions Research Center. This research was sponsored by the U.S. Department of Energy, Office of Energy Efficiency and Renewable Energy, Vehicle Technologies Program, with Ken Howden and Gurpreet Singh as the Program Managers.

References

[1] C. Ciardelli, I. Nova, E. Tronconi, D. Chatterjee, B. Bandl-Konrad, Chem Commun. (2004) 2718–2719.
[2] I. Nova, C. Ciardelli, E. Tronconi, D. Chatterjee, B. Bandl-Konrad, Catal. Today 114 (2006) 3–12.
[3] I. Nova, C. Ciardelli, E. Tronconi, D. Chatterjee, M. Weibel, Top Catal. 42 (2007) 43–46.
[4] M. Koebel, G. Madia, F. Raimondi, A. Wokaun, J. Catal. 209 (2002) 159–165.
[5] A. Grossale, I. Nova, E. Tronconi, D. Chatterjee, M. Weibel, J. Catal. 256 (2008) 312–322.
[6] A. Grossale, I. Nova, E. Tronconi, J. Catal. 265 (2009) 141–147.
[7] Y.H. Yeom, J. Henao, M.J. Li, W.M. Sachtler, E. Weitz, J. Catal. 231 (2005) 181–193.
[8] M.P. Ruggeri, A. Grossale, I. Nova, E. Tronconi, H. Jirglova, Z. Sobalik, Catal. Today 184 (2012) 107–114.
[9] P.S. Metkar, V. Balakotaiah, M.P. Harold, Catal. Today 184 (2012) 115–128.
[10] M. Iwasaki, H. Shinjoh, Appl. Catal. A: Gen. 390 (2010) 71–77.
[11] H. Sjövall, R.J. Blint, L. Olsson, Appl. Catal. B: Environ. 92 (2009) 138–153.
[12] M. Ruggeri, I. Nova, E. Tronconi, Top Catal. 56 (2013) 109–113.
[13] S.J. Schmieg, S.H. Oh, C.H. Kim, D.B. Brown, J.H. Lee, C.H.F. Peden, D.H. Kim, Catal. Today 184 (2012) 252–261.
[14] T.J. Toops, D.B. Smith, W.P. Partridge, Appl. Catal. B: Environ. 58 (2005) 245–254.
[15] T.J. Toops, M. Crocker, Appl. Catal. B: Environ. 82 (2008) 199–207.
[16] J.H. Kwak, R.G. Tonkyn, D.H. Kim, J. Szanyi, C.H. Peden, J. Catal. 275 (2010) 187–190.
[17] T. Venkov, K. Hadjiivanov, A. Milushev, D. Klissurski, Langmuir 19 (2003) 3323–3332.
[18] T. Hoost, K. Laframboise, K. Otto, Appl. Catal. B: Environ. 7 (1995) 79–93.

[19] J.W. London, A.T. Bell, J. Catal. 31 (1973) 96–109.
[20] K. Hadjiivanov, Catal. Lett. 68 (2000) 157–161.
[21] J. Szanyi, M.T. Paffett, J. Catal. 164 (1996) 232–245.
[22] K. Hadjiivanov, J. Saussey, J. Freysz, J. Lavalley, Catal. Lett. 52 (1998) 103–108.
[23] K. Hadjiivanov, E. Ivanova, M. Daturi, J. Saussey, J.-C. Lavalley, Chem. Phys. Lett. 370 (2003) 712–718.
[24] J.H. Kwak, J.H. Lee, S.D. Burton, A.S. Lipton, C.H. Peden, J. Szanyi, Angew. Chem. 125 (2013) 10169–10173.
[25] J. Szanyi, J.H. Kwak, H. Zhu, C.H. Peden, Phys. Chem. Chem. Phys. 15 (2013) 2368–2380.
[26] J.H. Kwak, H. Zhu, J.H. Lee, C.H. Peden, J. Szanyi, Chem. Commun. 48 (2012) 4758–4760.
[27] D.W. Fickel, R.F. Lobo, J. Phys. Chem. C 114 (2009) 1633–1640.
[28] M. Colombo, I. Nova, E. Tronconi, Catal. Today 151 (2010) 223–230.
[29] K. Hadjiivanov, H. Knözinger, B. Tsyntsarski, L. Dimitrov, Catal. Lett. 62 (1999) 35–40.
[30] J.-S. McEwen, T. Anggara, W. Schneider, V. Kispersky, J. Miller, W. Delgass, F. Ribeiro, Catal. Today 184 (2012) 129–144.
[31] M. Zamadics, X. Chen, L. Kevan, J. Phys. Chem. 96 (1992) 2652–2657.
[32] N.K. McGuire, C.A. Bateman, C. Scott Blackwell, S. Wilson, R.M. Kirchner, Zeolites 15 (1995) 460–469.
[33] A.F. Gualtieri, E. Passaglia, Eur. J. Mineral. 18 (2006) 351–359.
[34] B. Adelman, T. Beutel, G.-D. Lei, W. Sachtler, J. Catal. 158 (1996) 327–335.
[35] T. Beutel, B. Adelman, W. Sachtler, Appl. Catal. B: Environ. 9 (1996) L1–L10.
[36] F. Gao, E.D. Walter, E.M. Karp, J. Luo, R.G. Tonkyn, J.H. Kwak, J. Szanyi, C.H. Peden, J. Catal. 300 (2013) 20–29.
[37] J. Xue, X. Wang, G. Qi, J. Wang, M. Shen, W. Li, J. Catal. 297 (2013) 56–64.
[38] S.A. Bates, A.A. Verma, C. Paolucci, A.A. Parekh, T. Anggara, A. Yezerets, W.F. Schneider, J.T. Miller, W.N. Delgass, F.H. Ribeiro, J. Catal. 312 (2014) 87–97.
[39] M. Rivallan, G. Ricchiardi, S. Bordiga, A. Zecchina, J. Catal. 264 (2009) 104–116.
[40] A. Guzmán-Vargas, G. Delahay, B. Coq, E. Lima, P. Bosch, J.-C. Jumas, Catal. Today 107 (2005) 94–99.
[41] M. Colombo, I. Nova, E. Tronconi, Appl. Catal. B: Environ. 111 (2012) 433–444.
[42] F. Giordanino, P.N. Vennestrøm, L.F. Lundegaard, F.N. Stappen, S. Mossin, P. Beato, S. Bordiga, C. Lamberti, Dalton Trans. 42 (2013) 12741–12761.
[43] G. Centi, S. Perathoner, Appl. Catal. A: Gen. 132 (1995) 179–259.
[44] M.P. Ruggeri, T. Selleri, M. Colombo, I. Nova, E. Tronconi, J. Catal. 311 (2014) 266–270.